CARBON letters

Original Articles
Carbon Letters Vol. 21, 68-73 (2017)

Study of complex electrodeposited thin film with multi-layer graphene-coated metal nanoparticles

Young-Lae Cho[1], Jung-woo Lee[1], Chan Park[2], Young-il Song[1,3,♠] and Su-Jeong Suh[1,3,♠]

[1]School of Advanced Materials Science & Engineering, Sungkyunkwan University, Suwon 16419, Korea
[2]Department of Materials Science and Engineering, Pukyoung National University, Busan 48547, Korea
[3]Advanced Materials and Process Research Center for IT, Sungkyunkwan University, Suwon 16419, Korea

Article Info
Received 12 October 2016
Accepted 21 November 2016

♠Corresponding Author
E-mail: suhsj@skku.edu
physein01@skku.edu
Tel: +82-31-290-5641

Open Access
DOI: http://dx.doi.org/10.5714/CL.2017.21.068

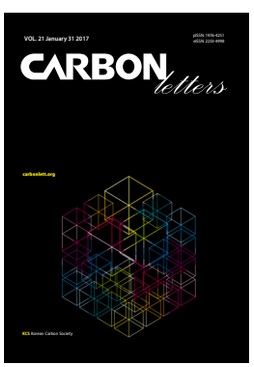

http://carbonlett.org

pISSN: 1976-4251
eISSN: 2233-4998

Abstract

We have demonstrated the production of thin films containing multilayer graphene-coated copper nanoparticles (MGCNs) by a commercial electrodeposition method. The MGCNs were produced by electrical wire explosion, an easily applied technique for creating hybrid metal nanoparticles. The nanoparticles had average diameters of 10–120 nm and quasi-spherical morphologies. We made a complex-electrodeposited copper thin film (CETF) with a thickness of 4.8 μm by adding 300 ppm MGCNs to the electrolyte solution and performing electrodeposition. We measured the electric properties and performed corrosion testing of the CETF. Raman spectroscopy was used to measure the bonding characteristics and estimate the number of layers in the graphene films. The resistivity of the bare-electrodeposited copper thin film (BETF) was 2.092×10^{-6} Ω·cm, and the resistivity of the CETF after the addition of 300 ppm MGCNs was decreased by 2% to ~2.049×10^{-6} Ω·cm. The corrosion resistance of the BETF was 9.306 Ω, while that of the CETF was increased to 20.04 Ω. Therefore, the CETF with MGCNs can be used in interconnection circuits for printed circuit boards or semiconductor devices on the basis of its low resistivity and high corrosion resistance.

Key words: complex electrodeposition, metal nanoparticles, multi-layer graphene-coated cu nanoparticles, electrical wire explosion process, corrosion resistance

1. Introduction

Electrodeposition recently has been widely used in various industries to coat metal substrates with thin films of different metals. However, thin films of different deposited metals may require unique properties that the substrate metal lacks. Therefore, the electrodeposition of metallic coatings containing nanoparticles has been of increasing interest in connection to electrodeposition applications to improve metal layer properties. In particular, the unusual optical, thermal, chemical, and physical properties of metal nanoparticles can be tailored by controlling the particle sizes and shapes.

Metallic nanoparticles and carbon-coated metal particles have been used extensively for various applications, such as energy storage materials, electrode pastes, printable inks, catalysts, ferrofluids, and biosensors [1-5]. Previous studies have shown that nanoparticles with surfactants can be suspended in electrolytes by agitation and then deposited as composites onto metals by electrodeposition [6]. Moreover, the electrodeposition of metallic coatings containing nanoscale particles can increase micro-hardness and corrosion resistance, modify growth to form nanocrystalline metal deposits, and change the reduction potential of metal ions [6-9]. By electrodeposition, controlled amounts of such particles can be embedded in the electrochemically produced solid phase of a coating, allowing special properties to be realized [7].

Nanoscale metal powders often become oxidized because they have high surface energies. Therefore, metal nanoparticles can form thin coating oxide layers, which degrade the properties of the particles. However, the introduction of a carbon layer can preserve the unique properties of metal layers and particles. Various methods to form such carbon layers on nanoscale metal powders have been reported, including arc-discharge, ion-beam sputtering, high-temperature heat treatment, electric explosion, and chemical deposition [10,11]. The electrical wire explosion technique has been especially common in producing carbon film-coated metal nanoparticles. With this technique, a high current is passed through a thin metal wire in air, ambient gases, or liquid media to create carbon-coated metal nanoparticles [12-15]. The metal powders must be dispersible and safe for application in devices for use in various industrial fields.

We have demonstrated the production of a complex-electrodeposited copper thin film (CETF) containing multilayer graphene-coated copper nanoparticles (MGCNs) by a typical electrodeposition method and determined the electrical and corrosion resistance properties of the films. We have also determined the growth mechanism of complex electrodeposition in a dispersion of metal nanoparticles in an electrolyte. Finally, we have verified the structure of the CEFT by experimental analysis.

2. Experimental

The MGCNs were fabricated by an electrical wire explosion process in a liquid medium of isopropyl alcohol (IPA) using copper (Cu) wire as a source material. In this electrical wire explosion setup, a thin Cu wire of 0.3 mm diameter was inserted between high-voltage and grounded electrodes, which were connected to an air gap voltage switch, and charged by a 0.05-μF capacitor bank from a high-voltage power source. A Cu wire of 12 mm length was exploded once and used in the experiment. A high voltage of 8.0 kV in 300 mL of the liquid solution was applied to the Cu wire for 90 explosions. We obtained MGCNs from the hybrid metal particles dispersed in the IPA by filtration. The separated MGCNs were cleaned several times in deionized water and dried for 30 min at 60°C in an oven [16].

Table 1 lists the composition and conditions used for the plating electrolyte. All solutions were commercially available (Atotech Co., Germany). 304 stainless steel plates (Nilaco Co., Japan) with dimensions of 5 cm × 5 cm × 0.1 mm were used as cathodes and Pt grids were used as anodes. The cathodes were prepared by polishing with sandpaper to a grade of 1500.

Table 1. Composition and conditions of plating bath

Chemical/parameter	Concentration/condition
$CuSO_4 \cdot 5H_2O$ (mol/L)	0.79
H_2SO_4 (mol/L)	0.305
HCl (mol/L)	0.000874
MGCNs (ppm)	100–300
Current density (mA/cm^2)	15
Magnetic stirring (rpm)	80
Temperature (°C)	~25

MGCNs, multilayer graphene-coated copper nanoparticles.

The current density for Cu plating was controlled at 1.5 A/cm^2 and electrodeposition was performed for 15 min at 25°C. The MGCNs were added to the Cu electrolyte solution at a concentration of ~300 ppm and then dispersed in the electrolyte solution using ultrasonic agitation for 10 min. Before and during electrodeposition, the bath was agitated using a magnetic stirrer at 80 rpm. The bare-electrodeposited copper thin film (BETF) and the CETF containing 300 ppm MGCNs were both ~4.8 μm thick.

Electrochemical impedance spectroscopy (EIS) is an effective technique for probing the features of chemically modified electrodes and for understanding electrochemical reaction rates and has been used in many studies [17]. The interfacial phenomena are modeled by the Randles and Ershler electronic equivalent circuit, as shown in Fig. 1a.

The faradaic impedance spectrum, known as a Nyquist plot, corresponds to the dependence of the imaginary resistance on the real resistance, and provides extensive information about the electric field interface and the electron transfer reaction. Nyquist plots commonly include a semicircle region lying on the axis followed by a straight line. The semicircle portion corresponds to the electron-transfer-limited process, while the straight line represents the diffusion-limited process. The Nyquist plot of the electrochemical system is shown in Fig. 1b [17].

The morphology and the size distribution of the MGCNs were characterized using high-resolution transmission electron microscopy with energy dispersive X-ray spectroscopy (HR-TEM with EDX, JEM-3010; JEOL Co., Japan) and dynamic light scanning (DLS; Otsuka Electronics Co., Japan). Phase analysis and chemical bonding analysis of the MGCNs were performed using X-ray diffraction (XRD; D8 ADVANCE, Bruker, USA), Raman spectral measurements with a laser excitation wavelength of 532 nm (Santerra, Bruker, USA), and X-ray photoelectron spectroscopy (XPS; ESCA2000, VG Microtech, UK). The surface morphology of the CETF was studied using a field emission scanning electron microscope (FE-SEM; Jeol JSM-700F, JEOL) with EDX. The resistivity of the electrodeposited Cu sheet was measured by a four-point probe (CMT-SR200N, AIT, Korea). Finally, chronoamperometry and EIS were performed by a potentiostat/galvanostat (VSP, Bio-Logic, France) with a saturated calomel reference electrode for electrochemical characterization.

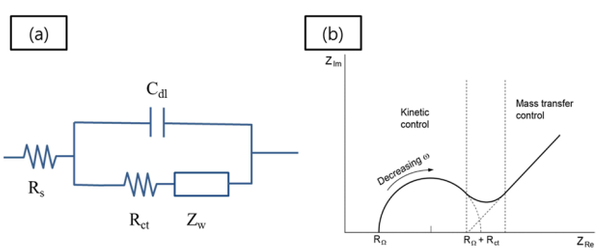

Fig. 1. (a) Schematic of circuit for corrosion resistance test. (b) Faradic impedance plot for corrosion resistance analysis on an electrochemical system.

3. Results and Discussion

Fig. 2a-c show transmission electron microscopy images of the MGCNs. These MGCNs were prepared in liquid IPA by the electrical wire explosion method, which created core-shell structured particles having Cu cores with multilayered graphene shells. In the case of the electrical explosion method, the energy applied to the wire caused it to vaporize within the IPA. The vaporized Cu then cooled rapidly to the temperature of the surrounding liquid media, resulting in condensation of Cu and crystallization of carbon from IPA molecular destruction onto the Cu particles. The MGCNs are formed with uniform spherical shapes of less than 40 nm diameter (Fig. 2a). Moreover, the multilayer graphene films are confirmed to be 3–5 layers thick, with a layer thickness of 0.34 nm each (Fig. 2b and c) [18-20]. Fig. 2d shows the Raman spectrum of the MGCNs. The peaks at 1348 cm^{-1}, 1586 cm^{-1}, and 2440 cm^{-1} are the D, G, and 2D peaks, respectively. The D and G peaks represent the graphene shoulder peaks. Next, the carbon surrounding the core was confirmed to be multi-layered graphene. The carbon layers form around the Cu particle at the time of the electrical explosion [21,22].

Fig. 3 shows the size distribution of the MGCNs, as determined using DLS. The MGCNs range from 83 nm to 270 nm in size with an average particle size of 107.4 nm. Although the MGCNs are shown to be less than 40 nm in Fig. 2, the DLS-measured particle size is larger. This different range in size can be explained by the aggregation of the MGCNs in solution [23-25].

Fig. 4 shows a FE-SEM surface image of the 300-ppm MGCNS-modified Cu thin film fabricated by the complex electrodeposition method. The growth of the Cu thin film occurs by the uniform and individual nucleation of Cu particles of 40 nm size for 1 s (Fig. 4a). As the growth of the Cu thin film increases, an individual Cu particle nucleates for 5 s before forming a thin film for 10 s (Fig. 4b and c). These particles were analyzed by EDX, revealing that they were composed of Cu; however, we found no images of MGCNs embedded in the CETF. We created a CETF with a thickness of 4.8 μm in 15 min. Fig. 4d shows the surface morphology of the CETF. It is similar to that of the inserted image of the surface morphology of the BETF.

The XRD pattern of the MGCNs is shown in Fig. 5a. The XRD pattern of the MGCNs shows high-intensity peaks at 43.36° (111), 50.52° (200), and 73.57° (220) corresponding to the crystal structure of face-centered cubic bulk Cu. The C peak of the MGCNs indicates that the low carbon solubility has a negligible effect on the Cu particles. Fig. 5b shows the wide-scan XPS spectrum for the MGCNs. The general spectrum shows a high-intensity peak at 284.4 eV (C 1*s*) and a low-intensity peak at 532.2 eV (O 1*s*). The two peaks at 932 eV (Cu $2p_{3/2}$) and 952

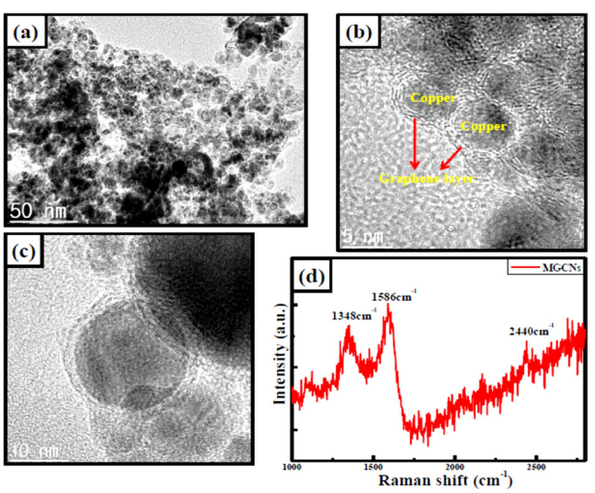

Fig. 2. Transmission electron microscopy images of the multilayer graphene-coated copper nanoparticles (MGCNs). (a) The size of the MGCNs is less than 40 nm. (b, c) The MGCNs were created using an electrical explosion method and have a core-shell structure with multi-layer graphene films. It was confirmed that there were 3–5 layers of graphene and the thickness of one layer was 0.34 nm. (d) Raman spectrum of the MGCNs. Raman shifts at 1348 cm^{-1}, 1586 cm^{-1}, and 2440 cm^{-1} are the D, G, and 2D peaks, respectively.

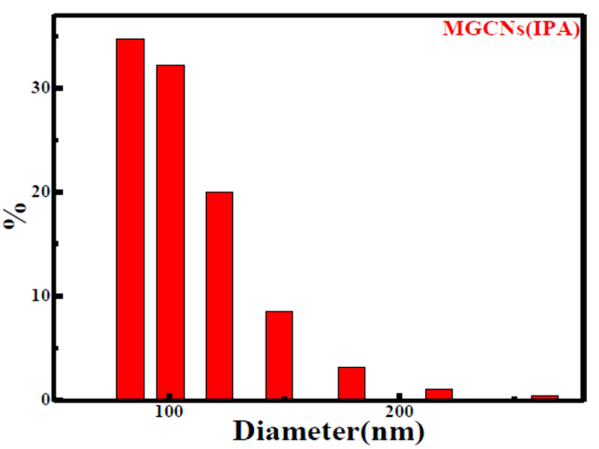

Fig. 3. Particle size distribution for multilayer graphene-coated copper nanoparticles (MGCNs) by DLS. IPA, isopropyl alcohol.

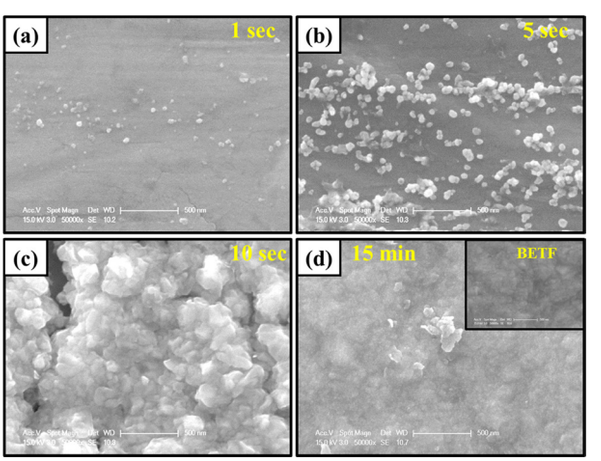

Fig. 4. Field emission scanning electron microscope image of the plated Cu surface. The surface morphology of 300 ppm multilayer graphene-coated copper nanoparticles added Cu complex-electrodeposited copper thin film (CETF) according to time are (a) 1 s, (b) 5 s, (c) 10 s, (d) 15 min, and (d) the surface morphology of the bare-electrodeposited copper thin film (BETF) inserted.

DOI: http://dx.doi.org/10.5714/CL.2017.21.068

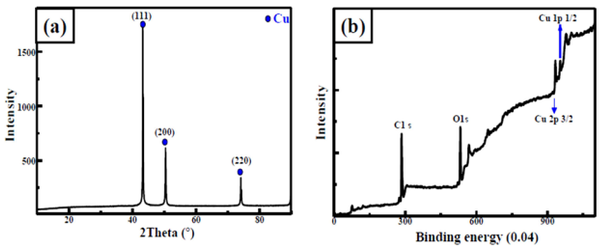

Fig. 5. (a) The X-ray diffraction patterns of the collected multilayer graphene-coated copper nanoparticles (MGCNs) using a 514 nm laser line. (b) General X-ray photoelectron spectroscopy scan of the MGCNs.

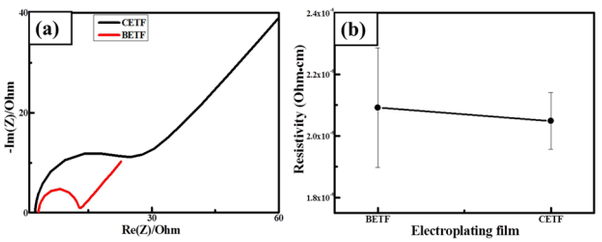

Fig. 6. Resistivity and corrosion resistance of the 300 ppm multilayer graphene-coated copper nanoparticle added Cu complex-electrodeposited copper thin film (CETF) and base Cu electrodeposition thin film. BETF, bare-electrodeposited copper thin film.

eV (Cu $2p_{1/2}$) indicate the formation of Cu-O chemical bonds. Therefore, we can that some copper oxide materials are formed; the MGCNs dominantly contribute to the C peak. The data clearly indicate that the graphene layer coating the Cu particles is protecting Cu from oxidation.

Fig. 6 shows the resistivity and EIS of the BETF and the MGCNs-modified CETF. The electrical resistivity of the plated Cu thin films is calculated based on the sheet resistance and the film thickness. The sheet resistance was measured at nine points and the average value was used as the resistivity. Fig. 6a depicts the experimental (solid line) and simulated (dot line) EIS results under various conditions. R_s is shown in the Nyquist plot as the X-intercept. The diameter of the circle corresponds to the resistance (R) of the combined R_{ct} and R_s; larger-diameter circles indicate the films have superior corrosion resistance [17].

The corrosion behavior changes with the addition of MGCNs, as shown in Fig. 6a. This shows that corrosion is closely related to changes in the crystal structure and film morphology. R_{ct} is increased from 9.306 Ω to 20.04 Ω, which decreases the corrosion current of the thin film; the corrosion rate of the thin film is therefore delayed with the addition of MGCNs. Fig. 6b shows the resistivity of the films. The samples showed resistivity of 2.09×10^{-6} Ω·cm for the BETF and 2.04×10^{-6} Ω·cm for the MGCN-modified CETF. In general, additives act as impurities, increasing the resistivity of films. However, the resistivity of the MGCN-modified CETF is demonstrated to decrease by ~2.5%. According to the corrosion resistance and resistivity results, this is associated with the change in crystal structure and surface morphology.

Fig. 7 shows the XRD patterns of the BETF and 300-ppm MGCNs-modified CETF. The magnitude of the (111) peak is significantly increased by the addition of the MGCNs. Using the

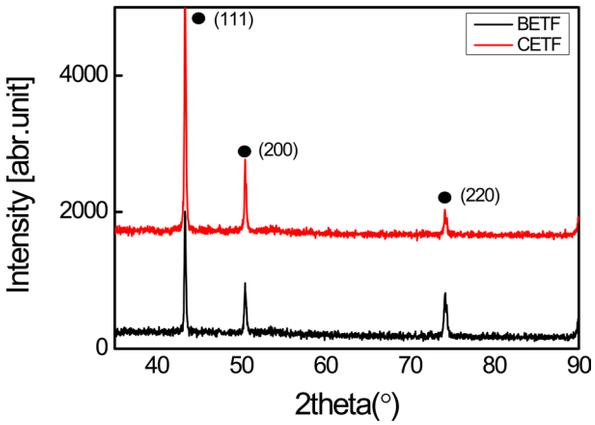

Fig. 7. Results of X-ray diffraction of the bare copper film and the 300 ppm multilayer graphene-coated copper nanoparticle added Cu complex-electrodeposited copper thin film (CETF). BETF, bare-electrodeposited copper thin film.

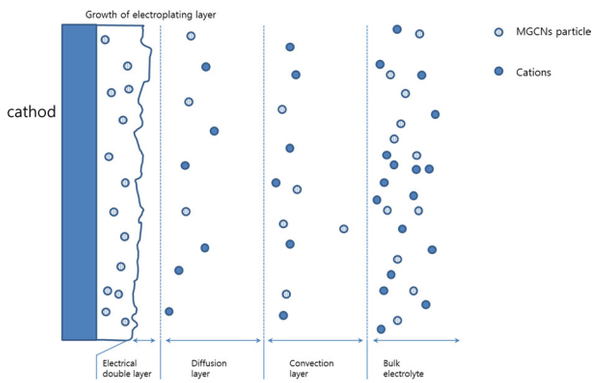

Fig. 8. Schematic of growing mechanism of the complex plating in multilayer graphene-coated copper nanoparticle (MGCN) added electrolyte solution.

Scherrer formula, we determined the grain size [26].

$$D_p = \frac{0.92\lambda}{\beta_1 / cos\theta} \quad (1)$$

Here, D_p = average crystallite size, β = line broadening in radians, θ = Bragg angle, and λ = X-ray wavelength. The grain sizes of the BETF and MGCN-modified CETF are 37.81 nm and 50.43 nm. As a result, the MGCN-modified CETF shows an increased (111) peak intensity because of the increased grain size. Therefore, we suggest that this caused the improvement of the corrosion resistance and resistivity. However, this mechanism remains unclear, because nanomaterials have previously been shown to possess different properties and characteristics compared to bulk materials. We propose that the MGCN-modified CETF has a lower resistivity and higher corrosion resistance because of the increased grain size in the complex bulk thin film and because of the anti-oxidation protection of the metal particles by the molecular barrier properties of the added graphene layers.

Finally, Fig. 8 shows a schematic illustration of the mecha-

nism of particle co-deposition onto a metal by electrodeposition. This is a common process that involves the co-deposition of particles into a growing metal matrix [9]. Between the electrolyte and the cathode, there are four layers, as shown in Fig. 8. The cations and powder are present within the bulk electrolyte. When plating is initiated, the cations and powder move to the diffusion layer through the convection layer. As a result, the Cu thin film is deposited through reduction that occurs at the cathode surface. In this case, the mechanism is based on the powder present around the cathode surface being plated with cations in the electrical double layer. Note that Fig. 8 is only a prediction; future studies are necessary to determine the exact mechanism.

4. Conclusions

In this study, MGCNs less than 40 nm in size were prepared by an electrical wire explosion method. These MGCNs were composed of Cu cores with multilayer graphene shells. By adding the MGCNs to the electrolyte solution for electrodeposition, a thin film with a thickness of ~4.8 μm was achieved. Through XRD and XPS analyses we demonstrated that the MGCNs protect Cu from oxidation. Moreover, the resistivity results confirmed that the MGCN-modified CETF had a resistance 2% lower than that of the BETF. This reduction in resistivity is attributed to the increase in the grain size, as indicated by the increase in the (111) peak intensity relative to that from the CETF. R_{ct} for the MGCNs-modified CETF, as measured by the EIS analysis, was increased from 9.306 Ω to 20.04 Ω, showing that the corrosion resistance is improved by the addition of MGCNs. The mechanisms underlying the improvements in resistivity and corrosion resistance by the co-deposition of MGCNs are not yet exactly understood. However, in the future, we plan to research the electrodeposition behavior, resistivity, and corrosion resistance of CETF depending on the concentration of MGCNs.

Conflict of Interest

No potential conflict of interest relevant to this article was reported.

Acknowledgements

This study was supported by the Basic Research Support Program (BRSP) of the National Research Foundation (NRF) of Korea, and by the Regional Innovation Center (RIC) of Korea, which is funded by the Ministry of Education (MOF, Grant No. 2013R1A1A2061254) and the Ministry of Trade, Industry and Energy (MTIE) of Korea. The research was also supported by the ITRC (Information Technology Research Center) support program (IITP-2016-H8501-16-1009) supervised by the IITP (Institute for Information & communications Technology Promotion) and the Technology Innovation Program (10049864, Embedded thin capacitor (pF/uF) development in PCB), which is funded by the Ministry of Trade, Industry & Energy (MI, Korea).

References

[1] Choi SUS, Eastman JA. ASME International Mechanical Engineering Congress & Exposition, San Francisco, CA (1995).

[2] Lu AH, Salabas EL, Schüth F. Magnetic nanoparticles: synthesis, protection, functionalization, and application. Angew Chem, **46**, 1222 (2007). https://doi.org/10.1002/anie.200602866.

[3] Garcia MA. Surface plasmons in metallic nanoparticles: fundamentals and applications. J Phys D Appl Phys, **44**, 283001 (2011). https://doi.org/10.1088/0022-3727/44/28/283001.

[4] Murphy CJ, Sau TK, Gole AM, Orendorff CJ, Gao J, Gou L, Hunyadi SE, Li T. Anisotropic metal nanoparticles: synthesis, assembly, and optical applications. J Phys Chem B, **109**, 13857 (2005). https://doi.org/10.1021/jp0516846.

[5] Crooks RM, Zhao M, Sun L, Chechik V, Yeung LK. Dendrimer-encapsulated metal nanoparticles: synthesis, characterization, and applications to catalysis. Acc Chem Res, **34**, 181 (2001). https://doi.org/10.1021/ar000110a.

[6] Low CTJ, Wills RGA, Walsh FC. Electrodeposition of composite coatings containing nanoparticles in a metal deposit. Surf Coat Technol, **201**, 371 (2006). https://doi.org/10.1016/j.surfcoat.2005.11.123.

[7] Musiani M. Electrodeposition of composites: an expanding subject in electrochemical materials science. Electrochim Acta, **45**, 3397 (2000). https://doi.org/10.1016/S0013-4686(00)00438-2.

[8] Daoush WM, Lim BK, Mo CB, Nam DH, Hong SH. Electrical and mechanical properties of carbon nanotube reinforced copper nanocomposites fabricated by electroless deposition process. Mater Sci Eng A, **513-514**, 247 (2009). https://doi.org/10.1016/j.msea.2009.01.073.

[9] Walsh FC, Ponce de Leon C. A review of the electrodeposition of metal matrix composite coatings by inclusion of particles in a metal layer: an established and diversifying technology. Trans IMF, **92**, 83 (2014). https://doi.org/10.1179/0020296713Z.000000000161.

[10] Athanassiou EK, Grass RN, Stark WJ. Large-scale production of carbon-coated copper nanoparticles for sensor applications. Nanotechnology, **17**, 1668 (2006). https://doi.org/10.1088/0957-4484/17/6/022.

[11] Kim B, Sigmund WM. Functionalized multiwall carbon nanotube/gold nanoparticle composites. Langmuir, **20**, 8239 (2004). https://doi.org/10.1021/la049424n.

[12] Cho CH, Park SH, Choi YW, Kim BG. Production of nanopowders by wire explosion in liquid media. Surf Coat Technol, **201**, 4847 (2007). https://doi.org/10.1016/j.surfcoat.2006.07.032.

[13] Dash PK, Balto Y. Generation of nano-copper particles through wire explosion method and its characterization. Res J Nanosci Nanotechnol, **1**, 25 (2011). https://doi.org/10.3923/rjnn.2011.25.33.

[14] Abdelkader EM, Jelliss PA, Buckner SW. Metal and metal carbide nanoparticle synthesis using electrical explosion of wires coupled with epoxide polymerization capping. Inorg Chem, **54**, 5897 (2015). https://doi.org/10.1021/acs.inorgchem.5b00697.

[15] Kotov YA. Electric explosion of wires as a method for preparation of nanopowders. J Nanopart Res, **5**, 539 (2003). https://doi.org/10.1023/B:NANO.0000006069.45073.0b.

[16] Lee JW, Kim TY, Cho YL, Na YI, Kim YS, Song YI, Suh SJ. Effect of liquid media on the formation of multi-layer graphene-synthesized metal particles. J Nanosci Nanotechnol, **15**, 9014 (2015). https://doi.org/10.1166/jnn.2015.11583.

[17] Wang J. Analytical Electrochemistry, 3rd ed., Wiley-VCH, Weinheim (2005).
[18] Cho C, Jin YS, Kang C, Lee GJ, Rhee CK. Preparation and analysis of Cu nanopowder by wire explosion in distilled water. Trans Korean Inst Electr Eng, **59**, 1272 (2010).
[19] Lee GH, Rhee CK, Kim WW, Kotov YA. Effect of atmospheric gas on the size and distribution of Cu nano powders synthesized by pulsed wire evaporation method. J Korean Powder Metall Inst, **11**, 210 (2004). https://doi.org/10.4150/KPMI.2004.11.3.210.
[20] Lee HM, Park JH, Hong SM, Uhm YR, Rhee CK. Fabrication and characterization of carbon-coated cu nanopowders by pulsed wire evaporation method. J Korean Powder Metall Inst, **16**, 243 (2009). https://doi.org/10.4150/KPMI.2009.16.4.243.
[21] Sato S. Graphene for nanoelectronics. Jpn J Appl Phys, **54**, 040102 (2015). http://dx.doi.org/10.7567/JJAP.54.040102.
[22] Wang S, Huang X, He Y, Huang H, Wu Y, Hou L, Liu X, Yang T, Zou J, Huang B. Synthesis, growth mechanism and thermal stability of copper nanoparticles encapsulated by multi-layer graphene. Carbon, **50**, 2119 (2012). https://doi.org/10.1016/j.carbon.2011.12.063.
[23] Singh BP, Nayak S, Nanda KK, Jena BK, Bhattacharjee S, Besra L. The production of a corrosion resistant graphene reinforced composite coating on copper by electrophoretic deposition. Carbon, **61**, 47 (2013). https://doi.org/10.1016/j.carbon.2013.04.063.
[24] Bennetta JA, Swainb GM. Investigating the nucleation and growth of electrodeposited Pt on polycrystalline diamond electrodes. J Electrochem Soc, **157**, F89 (2010). https://doi.org/10.1149/1.3430501.
[25] Brongersma SH, Kerr E, Vervoort I, Saerens A, Maex K. Grain growth, stress, and impurities in electroplated copper. J Mat Res, **17**, 582 (2002). https://doi.org/10.1557/JMR.2002.0082.
[26] Patterson AL. The Scherrer formula for X-ray particle size determination. Phys Rev, **56**, 978 (1939). https://doi.org/10.1103/PhysRev.56.978.